

**THE NUCLEAR REDDENING CURVE FOR ACTIVE
GALACTIC NUCLEI AND THE SHAPE OF THE INFRA-RED
TO X-RAY SPECTRAL ENERGY DISTRIBUTION**

C. MARTIN GASKELL and RENÉ W. GOOSMANN ¹

Department of Physics & Astronomy, University of Nebraska, Lincoln, NE 68588-0111

mgaskell1@unl.edu

rene.goosmann@obspm.fr

and

ROBERT R. J. ANTONUCCI and DAVID WHYSONG

Department of Physics & Astronomy, University of California, Santa Barbara, CA 93106

ski@spot.physics.uscb.edu

dwhysong@spot.physics.uscb.edu

Received _____; accepted _____

¹Present address: Observatoire de Paris, Section de Meudon, LUTH, Place Jules Janssen,
F-92195 Meudon Cedex, France

ABSTRACT

We present extinction curves derived from the broad emission lines and continua of large samples of both radio-loud and radio-quiet AGNs. The curves differ substantially from the standard Galactic extinction curve: they are significantly flatter in the UV than are curves for the local ISM. The reddening curves for the radio-quiet LBQS quasars are slightly steeper than those of the radio-loud quasars in the UV, probably because of additional reddening by dust further out in the host galaxies of the former. The UV extinction curves for the radio-loud AGNs are very flat. This is explicable with slight modifications to standard MRN dust models: there is a relative lack of small grains in the nuclear dust. We give a simple analytic fit to our “nuclear” reddening curve and give a tabulation for the wavelengths of major emission lines. Our continuum and broad-emission line reddening curves agree in both shape and amplitude, confirming that the continuum shape is indeed profoundly affected by reddening for all but the bluest AGNs. With correction by our generic extinction curve, all of the radio-loud AGN have continuous optical-UV spectra consistent with a single shape. We show that radio-quiet AGNs have the same intrinsic UV to optical shape over orders of magnitude in luminosity. We also argue that radio-loud and radio-quiet AGNs probably share the same underlying continuum shape and that the systematic differences between their observed continuum shapes are due to higher nuclear reddening in radio-selected AGNs, and additional reddening from dust further out in the host galaxies in radio-quiet AGNs. The luminosity dependence of both the optical and ultraviolet-to-optical spectral indices are completely consistent with the hypothesis that luminosity dependence of reddening dominates the correlations of the apparent UV to near IR continuum shapes with luminosity. Our conclusions have important implications for the modelling

of quasar continua and the analysis of quasar demographics.

Subject headings: galaxies:active — ISM:dust, extinction - galaxies:quasars:general — X-rays:galaxies — black hole physics — accretion: accretion disk

1. INTRODUCTION

Poor characterization of the extinction in Active Galactic Nuclei has been one of the biggest obstacles to understanding their nature. Without knowledge of the appropriate form and amplitude of the wavelength dependence of the extinction it is impossible to determine the true spectral energy distribution. It is also difficult to interpret emission-line spectra to diagnose conditions nears the black hole. There has been a long-standing controversy over the amount of reddening of AGNs. McKee & Petrosian (1974) argued against significant amounts of reddening in quasars on two grounds. The first was the apparent lack of the strong $\lambda 2175$ extinction hump (e.g., Pitman, Clayton, & Gordon 2000), and the second was the lack of curvature of the UV continuum. Cheng, Gaskell, & Koratkar (1991) found that the ultraviolet slopes for a wide variety of AGNs at high and low redshift, high and low luminosity, and differing radio types were essentially the same to within their measuring errors. They limited line-of-sight reddening to $E(B-V) \sim 0.1$ mag (assuming a Galactic reddening curve). In the optical, on the other hand, there is clear evidence at least for significant reddening in the host galaxy plane. De Zotti & Gaskell (1985) showed that both the lines and continua of radio-quiet AGNs (Seyfert galaxies) with axial ratio a/b are typically reddened by $E(B-V) \sim 0.2(a/b)$ mag. Also, unified models of both radio-loud and radio-quiet AGNs require significant dust extinction in a nuclear torus (tipped with respect to the spiral host; see Antonucci 1993) and this must produce detectable effects on spectra of both radio-loud and radio-quiet AGNs.

Reddening curves have been determined for the radio-quiet AGNs NGC 3227 (Crenshaw et al. 2001), and Ark 564 (Crenshaw et al. 2002) by assuming that they have the same underlying continuum as other, bluer AGNs. These reddening curves show little or no $\lambda 2175$ bump and rise *more* steeply in the far UV than the standard Galactic reddening curve (i.e., they resemble the reddening curve of the SMC). Crenshaw et al. (2001, 2002) argue that the dust in NGC 3227 and Ark 564 is outside the narrow-line regions and hence far removed from the nuclei. In this paper we determine mean reddening curves for large samples of radio-loud quasars and show that the reddening curves differ significantly both from those of NGC 3227 and Ark 564 and from any other previously-determined reddening curve. We then explore the significance of this result for our understanding of AGNs.

2. THE REDDENING CURVE

2.1. The Sample

Baker & Hunstead (1995) present composite Anglo-Australian Telescope optical and (rest-frame) UV spectra of 72 FR II radio quasars and broad line radio galaxies from the Molonglo Quasar Sample (MQS). The data have the advantages of being homogenous and being selected almost exclusively by radio-lobe flux, a nearly isotropic parameter. They also have broad optical/UV wavelength coverage, typically over a rest-frame wavelength range of typically $\sim 2000\text{\AA}$ to $\sim 5000\text{\AA}$ depending on redshift. Radio core-to-lobe flux ratios, \mathfrak{R} , were measured from 5 GHz VLA maps. Baker & Hunstead excluded a few AGNs from the sample because of abnormally strong absorption features, a lack of \mathfrak{R} -values, or a BL Lac type featureless spectrum. They grouped the AGNs into four subsets chosen according to \mathfrak{R} -values and radio structure, creating composite UV-optical spectra of 13-18 objects each. The four subsets are $\mathfrak{R} \geq 1$, $0.1 \leq \mathfrak{R} < 1$, $\mathfrak{R} < 0.1$ and Compact Steep Spectrum (CSS) radio sources. Baker & Hunstead (1996) also give mean line strengths for the four

subsets. In addition to the MQS AGNs we also considered the similar quality predominantly radio-quiet Large Bright Quasar Survey (LBQS) composite spectrum of Francis et al (1992).

2.2. Method and Justification of Method

Our continuum extinction curves are derived by division of pairs of composite continuum spectra, on the assumption that the intrinsic continua are the same. While routinely done for stars of a given spectral type, there is in principle a huge risk in applying this method to AGN. Stars with matched classifications almost certainly have intrinsically similar spectra, but there is no guarantee that one AGN composite is intrinsically similar to another. In fact for the AGN case, variability appears to affect the spectral shape so the intrinsic matches cannot be perfect for that reason alone. However, the averaging within the composites will greatly reduce the last problem. Note that our sub-samples are matched in radio-lobe power.

We also determined the reddening curve for the broad-line region (BLR) lines in the samples. In doing this we are again assuming that there are no intrinsic object-to-object BLR differences. This is certainly not true for individual objects but again we hope that the large number of AGNs in each subset minimizes the uncertainties introduced.

There are two very good pieces of evidence we will present that reddening (rather than intrinsic spectral differences) does in fact drive most of the observed spectral differences. The first is that a *single* reddening curve shape reconciles the shapes all four radio composites.

More importantly, we shall see that *the reddening curves derived from the continua and separately from the broad emission lines have nearly the same shape and amplitude.* Changing physical conditions in the BLR cannot mimic reddening when many lines are

considered together ².

As explained at the end of this paper, the validity of our conclusion will soon be tested in a simple robust manner: it predicts powerful infrared emission for the lobe-dominant radio-loud quasars, far exceeding that of the blue-selected PG radio-quiet quasars.

2.3. Results

2.3.1. Choice of Comparison Groups

There are four radio quasar samples considered in the paper: core dominant classical doubles, intermediate classical doubles, lobe-dominant classical doubles, and compact-steep-spectrum sources. Roughly speaking, the current wisdom is that the first three classes differ from one another only in orientation, while the last class comprises sources which are intrinsically different, in particular being much smaller physically.

We concentrate on two comparisons among the groups. First we compare the core-dominant vs the lobe-dominant sample. There is empirical and theoretical evidence that the latter are more reddened, so such a comparison should reveal the shape of that reddening.

The compact-steep-spectrum quasars are thought to range widely in orientation. They fill the parameter (viewing angle) space of all three groups of classical double radio quasars considered above. (note that the *edge-on* quasars are thought to be optically-obscured and to manifest themselves as radio-galaxies) Thus if we are to compare them to a subgroup of the classical doubles, it would be best to select the subgroup at intermediate orientation as we have done. One might compare them to a composite of all the classical doubles.

²However, a single line pair alone often gives ambiguous results – see Grandi (1982).

But restricting the comparison group to those at intermediate orientation has another very important advantage. Our two comparisons and thus our two reddening curves for the radio loud population are strictly independent of each other, with no objects in common. Thus their mutual agreement cannot be an artifact of interdependent samples.

2.3.2. *Reddening Curve Comparisons*

We derived relative reddening curves for two independent pairs of sub-samples of the four composite spectra given by Baker & Hunstead. We compare the $\mathfrak{R} \geq 1$ (“face-on”) sample with the $\mathfrak{R} < 0.1$ (“edge-on”) sample, and the $0.1 \leq \mathfrak{R} < 1$ (“intermediate-orientation”) sample with the CSS sample. We avoided prominent spectral features (like major broad or narrow emission lines and absorption troughs) or, in some cases, we made interpolations over residual absorption features and noisy regions of the spectra. We also determined the extinction curves for the BLR using the mean line strengths given in Table 1 of Baker & Hunstead (1996a,b). Because of the difficulty of measuring BLR strengths due to the wings of the lines the uncertainties are larger for the BLR lines than for the continua. In Figure 1 we show each of the $E(\lambda - V)$ curves normalized to $E(B - V) = 1$. Of course the uncertainty in the normalization in the optical introduces some uncertainty in the level of the UV curves.

The two continuum extinction curves, coming from the two totally independent data subsets, agree well especially since we have only matched the curves in the optical region rather than using a globally-optimal scaling to get the best overall match. It is important to note that the BLR extinction curve is also consistent with the two continuum curves.

All three reddening curves are extremely flat in the UV. This is very different behavior from the standard $R_V = 3.1$ Galactic reddening curve shown for comparison in Figure 1. It

is also very different from the Small Magellanic Cloud (SMC) reddening curve that has also been considered as a possible form of the wavelength dependence of the extinction in AGNs (Crenshaw et al. 2001, 2002),

A flat extinction curve implies large grain sizes relative to the wavelengths involved. We note in fact that Galactic reddening curves from regions with a large R_V value ($R_V \sim 5$), such as the line of sight to the star formation region Herschel 36, (Fitzpatrick & Massa 1988) do give flat UV extinction curves. The major difference between the Herschel 36 reddening curve and our radio-loud quasar curves is the absence of the $\lambda 2175$ absorption feature in our curves. For comparison we show a theoretical extinction curve with $R_V = 5.30$ (a good fit to the Herschel 36 line of sight) and a “normal” extinction curve (both curves are taken from Cardelli, Clayton & Mathis 1989, hereinafter CCM89).

Next we consider the predominantly radio-quiet (and blue-selected) LBQS survey objects. Figure 2 shows the relative reddening curve between the composite spectrum from Francis et al. (1992) and the relatively unreddened $\mathfrak{R} \geq 1$ composite of Baker & Hunstead (1995). Since the LBQS composite spectrum is rather noisy in the V-band, we did the normalization to $E(V - V) = 0$ and $E(B - V) = 1$ by doing a fit to the four data points with lowest frequencies. The resulting reddening curve is significantly steeper than the radio-loud reddening curves in Figure 1 but not quite as steep as the Galactic reddening curve, or the NGC 3227 and Akn 564 reddening curves of Crenshaw et al (2001, 2002). Again, there is the lack of the $\lambda 2175$ bump. In fact, there is an apparent dip in the reddening curve around the $\lambda 2175$ bump. This would be hard to understand physically unless there is a scattering component to the $\lambda 2175$ extinction feature. We suspect instead that this is due to a break down of our assumption that the intrinsic continua are the same for the samples. This could be a consequence of a difference in the UV Fe II emission. Part of the well-known Boroson & Green (1992) “eigenvector-1” correlations (which include differences between radio-loud

and radio-quiet AGNs) is variation in the Fe II emission and the Fe II emission is important in the so-called “small blue bump” (SBB) continuum around $\lambda^{-1} \sim 3.5$. De Zotti & Gaskell (1985) discuss the effects of Fe II on measurement of a $\lambda 2175$ absorption feature. Note that in deriving the reddening curves there is no reason to exclude SBB emission, which arises in the BLR; the dust affects it the same way as the BLR and continuum source. While $\lambda 2175$ has always been reported to be weak in AGNs it should be noted that De Zotti & Gaskell (1985) did find a correlation between their estimated reddening and published strengths of the $\lambda 2175$ feature (see their Table 3 and their Fig. 12) for dust in the host galaxy plane of Seyferts.

2.4. The Ratio of Total to Selective Extinction (R_V)

We estimated the R_V for our extinction curves by the standard method of extrapolating E_λ to $\lambda^{-1} = 0$. Actual measurements of E_λ in the IR are not available and would give inaccurate results anyhow because of the onset of IR emission from dust. Therefore, following the procedure of CCM89, we extrapolated to $\lambda^{-1} = 0$ by assuming that the IR reddening curve has the same shape as the Galactic curve of Rieke & Lebofsky (1985).³ To match Rieke & Lebofsky (1985) we convert our curves to A_λ/A_V using the following relation:

$$A_\lambda/A_V = \frac{A_\lambda - A_V}{A_V} + 1 = \frac{A_\lambda - A_V}{R_V \cdot E(B-V)} + 1 = \frac{1}{R_V} \cdot \frac{E(\lambda-V)}{E(B-V)} + 1.$$

We show one of our radio-loud A_λ/A_V AGN extinction curves together with the infrared data of Rieke & Lebofsky (1985) in Figure 3. We allow the Galactic curve to vary by a scale factor C (see CCM89). Assuming a similar shape for the AGN and Galactic

³The IR reddening is relatively low, and known reddening curves differ only slightly in that region, so this is probably safe

sample we obtain $R_V \sim 3.7$. For NGC 3227 Crenshaw et al. (2001) obtained $R_V = 3.2$ and for Akn 564 Crenshaw et al. (2002) obtained $R_V = 3.1$. Both of these are very close to the Galactic value, but again these Seyfert curves likely refer to a non-nuclear environment.

CCM89 show that the main variations in Galactic optical to UV extinction laws are a function of only one parameter: R_V . Using their functions for the radio-loud reddening curve we obtain $R_V = 4.1$ from the optical to near UV extinction curves and $R_V = 5.5$ from the far UV. For the LBQS reddening curve we obtain $R_V = 3.2$ and $R_V = 3.8$ respectively.

All three methods of determining R_V (IR extrapolation, UV/optical, and far-UV) give values of R_V for our radio-loud curves significantly greater than the canonical Galactic value of 3.1. The far-UV estimate has the smallest formal uncertainty.

Some additional support for the flat shape of our reddening curves in the UV comes from the lack of luminosity dependence of UV slopes found by Cheng et al. (1991) and the sharp upper limit to the $\lambda 4220/\lambda 1460$ ratio found by Malkan (1984). Ward et al. (1987) argue that all AGN continua are the same and that differences are due to reddening and host galaxy starlight contamination.

3. THE CONTINUUM SHAPE AND DEGREE OF REDDENING IN AGNS

In deriving the extinction curves for the radio quasars in the previous section, we started by assuming that the optical/UV-continuum shapes were the same *for each pair* of composites. This by construction leads to inferred intrinsic spectra which match each other for each pair. But what is *not* true by construction, and what argues for a rather generic reddening law, is that the two continuum extinction curves, derived from independent data, agree with each other in shape. More remarkably the continuum reddening curves for each pair agree in both shape and amplitude with curves derived from the *emission*

lines for both pairs of composites. Again this is not true by construction but argues for a correct and generic extinction law. See Fig 1 for the evidence. To summarize: both independent continuum pairs lead to the same extinction curve, and for each pair of continuum composites, the corresponding emission lines produce extinction curves which agree in shape and amplitude.

There is already evidence for a universal spectral energy distribution in radio quiet AGN. In Fig. 4 we show the $\lambda 1600/\lambda 4220$ spectral index, α_{UV0} (for $F_\nu \propto \nu^{-\alpha}$), for radio-quiet AGNs in three luminosity bins. We have calculated these from data in Malkan (1984) and references therein. We only show spectral indexes for objects with simultaneous or nearly simultaneous UV and optical observations. The observations were already corrected for Galactic reddening using $E(B-V)$ -values from Burstein & Heiles (1982) and assuming a standard Galactic reddening curve.

For the highest luminosity sample ($|\log L| > 30.5$) the mean α_{UV0} is 0.54 and the standard deviation is only 0.064. If this small dispersion is due to reddening it corresponds to $E(B-V) \sim 0.06$ assuming a reddening curve like our Fig. 1 or less than 0.02 if we assume a standard Galactic reddening curve. Thus, as was argued by Malkan (1984), the intrinsic extinction in these high-luminosity AGNs is probably very low.

For the radio-quiet AGNs with $29 < |\log L| < 30.5$, the important thing to note is that the *cutoff at $\alpha_{UV0} \sim 0.45$ is the same*. Both reddening and contamination by starlight from the host galaxy will increase α_{UV0} . For ($|\log L| < 29$ we see again that *there is the same cutoff at $\alpha_{UV0} \sim 0.45$* . As noted by Malkan (1984) the constancy of the cutoff slope in the face of a difference in the mean slope can be totally explained by increasing the host galaxy contamination and reddening. The cutoff at $\alpha_{UV0} \sim 0.45$ is presumably the unreddened value. *It is remarkable that this is the same over more than 4 orders of magnitudes in luminosity*. It would be hard to explain the increasing spread in spectral

index with decreasing luminosity as an *intrinsic* luminosity effect given that the cutoff is independent of luminosity.

For low-redshift, radio-loud quasars, Netzer et al. (1995) showed that there is a correlation between the observed $Ly\alpha/H\beta$ line ratios and the $\lambda 1216/\lambda 4861$ continuum flux ratios. This is evidence for radio-loud quasars having similar unreddened continuum shapes and similar hydrogen-line ratios. The bluest $\lambda 1216/\lambda 4861$ flux ratio on the reddening vector in their Fig. 6 is 8.7. This implies $\alpha_{UV0} \sim 0.44$ and supports the idea of a universal $\alpha_{UV0} \sim 0.45$. However, Bechtold et al. (1996) found a similar correlation (for the same wavelength range) for high-redshift predominantly radio-quiet AGN but the blue end of their reddening vector gives $\alpha_{UV0} \sim 0.2$. Baker et al. (2002) found that AGNs with steeper optical continua have stronger absorption lines. This means that there is more gas along the line of sight and this is consistent with there being more dust too.

Assuming that the bluest AGNs have $\alpha_{UV0} = 0.45$ and adopting our radio-loud-AGN reddening curve the mean reddenings (E(B-V)) of the four Molongo samples, going from “face-on” to CSS are, 0.29, 0.34, 0.71, and 0.98 mag. (with formal relative uncertainties of about ± 0.06). If the “face-on” sample is assumed to be unreddened then the mean reddenings are 0.00, 0.05, 0.41, and 0.69 magnitudes respectively, but this requires the unreddened $\alpha_{UV0} = 0.70$. We consider this highly unlikely since we get flatter (bluer) *observed* spectral indices from the Netzer et al. (1995) measurements. Since the reddening curve for the predominantly radio-quiet LBQS sample appears to be different, we derived the reddening from the long wavelength region (i.e., the optical) of the spectrum only. This give a mean E(B-V) ~ 0.30 mag (i.e., similar to the face-on Molongo radio-loud AGNs) if we assume that the unreddened $\alpha_{UV0} = 0.45$. Ward & Morris (1984) got E(B-V) ~ 0.3 for NGC 3783; Crenshaw et al. (2001) got a total E(B-V) of 0.20 for NGC 3227; and Crenshaw et al. (2002) got a total E(B-V) of 0.17 for Ark 564. All three of these are in the range

considered here.

Needless to say the lower apparent reddenings of radio-quiet, and hence usually optically-selected, AGNs must be strongly influenced by selection effects. It would be interesting to study the reddenings of X-ray selected samples of radio-quiet AGNs.

It should be noted that after de-reddening with our reddening curve, there is no difference between the spectral energy distribution of CSS sources and other AGNs. The apparent weakness of the SBB in CSS sources is simply a consequence of the high degree of reddening and the shape of the reddening curve which has its greatest curvature at the position of the SBB. Our reddening curve might similarly explain the unusual spectral shapes of some broad-absorption line quasars without the need to invoke partial covering (see Hall et al. 2002).

4. LUMINOSITY DEPENDENCE OF REDDENING

Assuming, as we have argued in the previous section, that the intrinsic continuum really is independent of luminosity, we can use our “AGN” reddening curve to investigate the luminosity dependence of the reddening. In Fig. 5 we show the luminosity dependence of the reddenings calculated from the UV to optical slope (as discussed in the previous section), and from the optical $\lambda 4200$ to $\lambda 7000$ slopes given by Mushotzky & Wandel (1989). It should be noted that the Malkan (1984) and Mushotzky & Wandel (1989) samples are two different heterogenous samples. We have assumed that the spectra are unreddened for the highest luminosities. The error bars are the errors in the means ($\sigma/\sqrt{(n)}$).

The first thing to notice from Fig. 5 is that the mean reddenings derived by the two methods and from two different samples are in agreement. This would not be the case had we used a standard galactic reddening curve; the reddenings derived from the UV-optical

slope (the solid squares) would then be more than a factor of two lower. Such differences as there are between the optical-only and UV-optical reddenings could be due to departures from our reddening curve (e.g., because of reddening by additional extra-nuclear dust), but they could equally well be due to differences in the samples. The Malkan (1984) sample is predominantly optically selected, and hence biased towards lower reddening objects; the larger Mushotzky & Wandel (1989) includes a large fraction of radio-loud, and thus radio-selected AGNs.

The second thing to notice is that the reddenings derived by both methods show a monotonic increase with decreasing luminosity. Mushotzky & Wandel (1989) attributed the steepening of the optical slope as being due to intrinsic differences in the spectral shapes, perhaps due to differing black hole masses and accretion rates (Wandel & Petrosian 1988). However, we can accurately predict the luminosity dependence of the optical slope in Mushotzky & Wandel (1989) entirely from the UV-optical reddening by using our reddening curve. We are not ruling out the possibility that there are luminosities in the intrinsic (de-reddened) continuum shape, but before these can be found, the dominating effect of the reddening has to be allowed for.

Variations in the degree of reddening from object to object naturally explain the spread in continuum shapes at a given luminosity. In Fig. 4 it can be seen that as the mean spectral index increases, so does its spread. If the continua are unreddened and the differences in continuum shape were real, perhaps due to differences in black hole mass and accretion rate, the wide spread in spectral index at lower luminosity is hard to understand.

5. THE RELATIONSHIP BETWEEN THE X-RAY AND OPTICAL EMISSION

5.1. Luminosity dependence of L_X/L_{opt}

It is long been known that the observed ratio of X-ray to optical luminosity is a decreasing function of optical (or UV) luminosity (Reichert, Mason, & Bowyer 1981, Zamorani et al. 1981, Avni & Tananbaum 1982, Kriss & Canizares 1985) with $L_X \propto L_{opt}^{0.70-0.85}$. This has generally been attributed to luminosity-dependent physical conditions in the AGNs themselves. In contrast to the relationship between L_X and L_{opt} , Malkan (1984) showed that $L_X \propto L_{IR}$. Mushotzky & Wandel (1989) reconciled these results by showing that the dependence of L_X on the luminosity at longer wavelengths depends on where the longer wavelength luminosity is measured. We believe instead that the L_X/L_{opt} ratio appears to vary simply because the greater extinction in lower luminosity objects causes the optical luminosity to appear to be lower than it really is. We quantitatively tested this by using $L_X \propto L_{opt}^a$, to predict the observed optical luminosity, then assuming that the intrinsic optical luminosity was proportional to L_X and using this to predict the reddening using our reddening curve. The luminosity dependence of the reddening seen in Fig. 5 is well matched with $a \sim 0.8$. Going in the other direction and assuming the luminosity dependence in Fig. 5, we predict that there should be some curvature in the L_X vs. L_{opt} plot. This should be detectable with well-defined samples.

5.2. Dependence of L_X/L_{opt} on Radio-loudness

Zamorani et al (1981) reported that radio-loud AGN are about three times as luminous in X-rays as radio-quiet AGN of the same observed optical luminosity. According to the arguments of the present paper, much of this difference must result from a denominator

in L_X/L_{opt} reduced by dust absorption. A factor of three corresponds to a difference in $E(B-V)$ of $\sim 0.25 - 0.35$ (depending on R_V). This is similar to the radio-loud/radio-quiet differences we find in optical absorption using our reddening curve (see above).

This is not the whole story however, because Zamorani et al (1981), Kembhavi (1994), Shastri (1997), and Brinkmann et al 1997, among others have argued that there is at least some contribution to the L_X/L_{opt} difference because the numerator is enhanced by a beamed component in the radio-loud objects with strong cores. The clinching argument here is that core-dominant objects often have harder X-ray spectra (Brinkmann et al. 1997), heralding the arrival of a new spectral component, but this observational effect is modest in size and ubiquity. We note that Sambruna, Eracleous, & Mushotsky (1999) find that X-ray slopes are similar for radio-loud and radio-quiet AGNs when the samples are matched in luminosity.

A quantitative assessment of the relative importance to the enhanced L_X/L_{opt} in radio-loud AGN of X-ray beaming and optical absorption is far beyond the scope of this paper. We simply state here that if we are correct, a significant part of the higher average L_X/L_{opt} in radio-loud AGN must be due to a denominator diminished by optical absorption in many cases, and this must be accounted for as well as the beaming.

6. DISCUSSION

6.1. Evidence for Larger Grain Sizes

The simplest explanation of the flat UV extinction curves we find is that small grain sizes are depleted relative to the grain-size distribution in our galaxy. There is other evidence for depletion of small grains. It has long been known that the optical extinction in AGNs is considerably less than is predicted by the X-ray column densities (Maccacaro,

Perola & Elvis 1982, Reichert et al. 1985). By comparing the reddening of optical and infrared broad lines and the X-ray absorbing column density Maiolino et al. (2001) find that the $E(B-V)/N_H$ ratio is nearly always lower than the Galactic values by a factor ranging from ~ 3 up to ~ 100 . They argue that this cannot be due to conversion of refractory elements to the gas phase but is instead caused by larger grains. Sambruna et al. (2002) find that approximately 50% of BLRGs have columns of cold gas comparable to the columns detected in NLRGs. This suggests that the small grains are depleted in gas swept off the torus.

The silicate feature at $9.7\mu m$ observed in the mid-IR spectra of many Galactic sources is absent in the average ISO spectrum of a sample of Seyfert 2 galaxies obtained by Clavel et al. (2000). Maiolino, Marconi, & Oliva (2001a) conclude that the most likely explanation of this is that dust in the circumnuclear region of AGNs is predominantly composed of large grains that do not contribute to the feature at $9.7\mu m$. Imanishi (2001) has argued from the probable shape of the IR L and M' band extinction curve that it is due to large grains.

There are other good arguments that small grains are severely depleted in gas swept off the torus. On the observational side, we are confident that free electrons sometimes dominate the scattering above the torus (Miller, Goodrich, & Goodrich 1991 ApJ 378, 47; Ogle et al 2003). Small grains have orders of magnitude greater scattering efficiency per gram of ionized Galactic interstellar medium compared with electrons, so they must be very thoroughly eliminated for electrons to dominate. From a theoretical standpoint too this gas very close to the sublimation radius can lose its small grains easily, by e.g. single-photon heating.

6.2. Modeling Extinction Curves for AGN

Mathis, Rumpl & Nordsieck (1977, MRN) suggested a standard galactic dust composition. In this model there are two sorts of grains with differing optical properties: carbonaceous or “graphite” grains, making up 37.5% and “astronomical silicate” making up 62.5%.

Weingartner & Draine (2001) developed the MRN model to construct size distributions for carbonaceous and siliceous grain populations in different regions of the Milky Way, LMC, and SMC. They present distributions that reproduce the observed extinction through various lines of sight. The $\lambda 2175$ feature is caused predominantly by *small* carbonaceous grains. Inspection of their results shows that extinction curves such as we find can be naturally explained by a relative lack of both small carbonaceous and small siliceous grains.

We modelled our AGN extinction curves using a computer code which calculates extinction cross sections from Mie theory. Such a code is given by Bohren & Huffman (1983). It is based on the solution of the Maxwell equations for radiation scattering off a spherical grain with defined radius a and dielectric constant ϵ . A graphite grain has differing optical properties for radiation propagating parallel or perpendicular to the symmetry axis of the crystal. The model takes care of this difference by using two different kinds of graphite grains, $G_{r_{\parallel}}$ and $G_{r_{\perp}}$. Considering three spatial dimensions there has to be twice as much $G_{r_{\perp}}$ as $G_{r_{\parallel}}$. In the standard MRN model the number density $n(a)$ of grains with radius a follows a $n(a) \sim a^{\alpha_s}$ law, with $\alpha_s = -3.5$, minimum grain size $a_{min} = 0.005\mu m$ and maximum grain size $a_{max} = 0.250\mu m$. Based on this grain composition MRN were able to compute the standard extinction curve for our Galaxy. Further details of our procedures can be found in Goosmann (2002).

We recalculated the standard extinction curve and then varied the dust composition, grain size limits and α_s . We found that the slope of the UV extinction curve tends to be

determined by a_{min} whereas the upper limit of $E(\lambda - V)$ varies more with α_s . In Fig. 6 we show a fit to our reddening curve. In order to achieve good agreement we lowered the abundance of graphite to 20% of the graphite/silicate mixture. In addition to this we raised a_{min} to $0.005\mu m$ and α_s to -2.05 . We lowered a_{max} to 0.200 . These changes could be explained by the better resistance of larger grains to destruction processes.

It is hard to explain why the fraction of carbonaceous dust is lower than in the MRN model since graphite actually has a higher sublimation temperature than silicate. The hard quasar radiation should preferably destroy silicate. This might be a limitation of our model where the only way to lower the $\lambda 2175$ feature is by decreasing the carbon abundance. In reality there might be another carbonaceous substance, such as PAH molecules, not included in our modelling, which is predominantly producing the $\lambda 2175$ feature.

We have made no attempt to model the reddening curve we found for radio-quiet AGNs because we suspect that the differences between this and the radio-loud reddening curve are caused by additional reddening further out in the host galaxy while the “nuclear” dust is similar. The dust further out would have more “Galactic” properties than the nuclear dust.

It should be noted that our “nuclear” reddening curve is for external line of sight reddening of a single point source. This is quite different from the case of starburst galaxies (Calzetti, Kinney, & Storchi-Bergmann 1994) where the dust is mixed in with multiple sources, each with different extinctions, and where geometrical effects in the complex environment affect the shape of the reddening curve. Those effects can eliminate the strong spectral curvature and exponential cutoff otherwise mandated by the usual reddening curves. In our case there are no exponential cutoffs despite the extinction being in the *foreground*.

6.3. Mechanisms for Depleting Small Grains

There are many mechanisms that can selectively destroy small grains. Gas in the outer regions of dense clouds in our galaxy are observed to have a higher relative abundance of larger grains (Mathis 1990) and this is believed to be due to coagulation of smaller grains. Absorption of a single X-ray photon will eliminate grains of radius $< 10\text{\AA}$ and deplete grains several times larger than this (Laor & Draine 1993). Small grains have a shorter lifetime due to thermal sputtering (Draine & Salpeter 1979). Smaller grains can also be efficiently destroyed by acquiring a high positive charge from the photoemission of electrons in the intense hard radiation field of AGNs (Draine & Salpeter 1979; Chang, Schiano, & Wolfe 1987). The high positive charge of large grains will also suppress thermal sputtering. If the AGN is not radiating far below the Eddington limit, grains will be efficiently accelerated away from the black hole. The ratio of radiative acceleration to gravitational acceleration is $\propto a^{-1}$, where a is the grain radius, so smaller grains will be expelled faster (see Draine & Salpeter 1979). The faster moving grains will also be subject to enhanced sputtering (Laor & Draine 1993).

6.4. Continuum Variability

In section 3 we have presented evidence for similarity of the average continuum shapes of a wide variety of AGNs. We are not, however, arguing for a precisely standard spectral energy distribution. It is widely reported that as AGNs vary $\alpha_{UV\text{O}}$ changes, being steeper in low states (e.g., Perola et al. 1982). However, much of the observed effect derives from a constant component from the host galaxy. Also contributing is the SBB atomic feature, which responds to continuum changes with reduced amplitude and a time delay; Korista & Goad (2001) recently showed that atomic continua can cover a much wider spectral region than just the SBB.

On the other hand, small delays have been reported between the UV flux and the optical (Collier et al. 1998, 2001; Kriss et al. 2000; Collier 2001, Oknyanskij et al. 2002; Gaskell et al., 2003). While there have been cases of reported steepening of the UV spectrum as AGNs have varied it is notable that in the case of Fairall 9 *the UV continuum slope stayed the same* at 0.46 ± 0.11 while the UV flux changed by a factor of over 20 (Clavel, Wamsteker, & Glass 1989).

Where the continuum does steepen as it fades it is possible that the extinction has changed (Barr 1982). If this is the case it would be due to compact dust clouds moving across the line of sight. There is support for this idea from the frequently-seen variations in X-ray column densities on timescales of less than a year (e.g., Risaliti, Elvis, Nicastro 2002), and the temporal variations in the position angles of the polarizations of broad lines in AGNs (e.g., Goodrich 1989, Martel 1998) which imply motions of the scattering dust clouds near the broad line region. More directly, Goodrich (1989) showed that the Balmer decrements and continuum slopes change simultaneously in a way consistent with varying reddening.

However changing extinction is far from the whole story of variability since the X-rays vary and often correlate with the optical/UV (see Gaskell & Klimek 2003 for review).

7. CONCLUSIONS

If our reasoning is correct, we can draw several important conclusions about AGNs.

1. The reddening curve for radio-loud AGNs has a fairly universal and unprecedented shape, being quite flat in the UV but selective in the optical.
2. The observed reddening of radio-quiet quasars is somewhat more selective in the UV relative to the optical, compared with radio-loud AGNs but this could well be because

of additional dust far out in the host galaxy.

3. Even though most well-studied quasars show no UV curvature, most of their light energy is in fact absorbed.

4. The flat nuclear reddening curve in the UV can be straightforwardly explained by grain destruction depleting the number of small grains, a notion consistent with many arguments in the literature.

5. The normalization (average amount of extinction) for lobe-dominant quasars on average decreases with radio core dominance, as anticipated by Baker et al (1997) and Baker and Hunstead (1995 ApJ 452, L95). There is powerful evidence from radio astronomy that this means absorption increases with line-of-sight inclination to the radio jets, as expected qualitatively in the standard “unified model” (Wills 1999).

6. Compact Steep-Spectrum (CSS) radio quasars have the same type of extinction curve and high reddening.

7. The continuum shapes of all but the bluest quasars are affected by reddening, and are intrinsically similar to those of the bluest quasars.

8. The average reddening decreases substantially with increasing luminosity.

9. The luminosity dependence of extinction explains most or all of the luminosity dependence of L_X/L_{opt} , and the variation of this dependence with the choice of optical wavelength.

10. Differences in reddening are also a major factor in the difference in L_X/L_{opt} between radio-loud and radio-quiet AGNs.

11. If they are correct many of these results are of vital importance for demographic studies (intrinsic luminosity density of AGN in the universe), and for modelling the crucial

BBB continuum component of AGN.

The most satisfying thing about the results from this paper are they are readily and robustly testable. The nearly unequivocal prediction is that radio-loud quasars are generally powerful thermal radiators. This is especially true for those with steep optical slope, despite their general lack of exponential UV cutoffs as expected in the case where small grains are present. While the exact infrared luminosities are model-dependent, only predictable statistically, and far beyond the scope of this paper, they should generally be energetically very important and often dominant. The one obvious caveat is that the optical/UV radiation may be intrinsically emitted anisotropically, as has been argued on other grounds by Miller, Goodrich, & Mathews (1991) among others. This could reduce the amount of re-processed radiation.

We are grateful to Mark Bottorff, Patrick Hall, Ari Laor, John Mathis, Dick McCray, Rita Sambruna, Joe Weingartner, & Adolf Witt for useful comments and discussion. This research was supported in part by NSF grant AST-0098719 and by the Hans-Böckler-Stiftung.

A. AN AGN EXTINCTION CURVE

In Table A1 we give an average extinction curve for the optical and the UV waveband. It is based on Fig. 1 and we have tabulated it at the wavelengths of major emission lines as well as the B and the V band in table 1.

The reddening curve can be represented analytically by the following functions of $x = \lambda^{-1}$ in μm^{-1} :

$$A_\lambda/A_V(x) = -0.9500 + 1.7002x - 0.4049x^2 + 0.0318x^3, \quad 1.25\mu m^{-1} \leq x < 3.71\mu m^{-1},$$

$$A_\lambda/A_V(x) = 1.3755 + 0.0089x, \quad 3.71\mu m^{-1} \leq x \leq 8\mu m^{-1}.$$

This analytic fit is shown in Fig. 6 after conversion to $\frac{E(\lambda-V)}{E(B-V)}$ using $R_V = 4.8$. This R_V value is the arithmetic middle of the optical/UV and the far UV value derived after CCM89 from our radio-loud reddening curve (see section 2.4).

REFERENCES

- Antonucci, R. R. J. 1993, *ARA&A*, 31, 473
- Antonucci R. R. J. 2002, in *Astrophysical Spectropolarimetry*, eds. J. Trujillo-Bueno, F. Moreno-Insertis, & F. Snchez (Cambridge: Cambridge Univ. Press) p. 151.
- Antonucci R. R. J. et al. 1996, *ApJ*, 472, 502
- Avni, Y.; Tananbaum, H. 1982, *ApJ*, 262, L17
- Baker, J. C., et al. 1997, *MNRAS* 286, 23
- Baker, J. C., & Hunstead, R. W. 1995, *ApJ*, 452L, 95
- 1996a, *ApJ*, 461L, 59 (Erratum)
- 1996b, *ApJ*, 468L, 131 (Erratum)
- Baker, J. C., Hunstead, R.W., Athreya, R. M., Barthel, P. D., de Silva, E., Lehnert, M. D., & Saunders, R. D. E. 2002, *ApJ*, 568, 592
- Barr, P. 1982, in *ESA 3rd European IUE Conf.* p. 559
- Bechtold, J., Shields, J., Rieke, M., Ji, P., Scott J., Kuhn, O., Elvis, M., & Elston, R. 1997, in *ASP Conf. Ser. 113, Emission Lines in Active Galaxies: New Methods and Techniques*, ed. B. M. Peterson, F.-Z. Cheng, & A. S. Wilson (San Francisco: ASP), 123
- Bohren C. F. & Huffman D. R., “Absorption and Scattering of light by small particles” (Wiley & Sons inc.)
- Brinkman, W., Yuan, W, & Siebert, J 1997, *A&A*, 319, 413
- Burstein, D., & Heiles, C. 1982 *AJ*, 87, 1165

- Calzetti, D., Kinney, A. L., & Storchi-Bergmann, T. 1994, *ApJ*, 429, 582.
- Cardelli, J. A., Clayton G. C., & Mathis, J. S. 1989, *ApJ*, 345, 245 (CCM89)
- Cheng, F. H., Gaskell, C. M., & Koratkar, A. P. 1991, *ApJ*, 370, 487
- Clavel, J., Schulz, B., Altieri, B., Barr, P., Claes, P., Heras, A., Leech, K., Metcalfe, L., & Salama, A. 2000, *A&A*, 357, 839
- Clavel, J., Wamsteker, W., Glass, I. S., 1989, *ApJ*, 337, 236
- Chang, C. A., Schiano, A. V. R., & Wolfe, A. M. 1987, *ApJ*, 322, 180
- Collier, S. J. 2001, *MNRAS*, 325, 1527
- Collier, S. J., et al. 1998, *ApJ*, 500, 162
- Collier, S. J., et al. 2001, *ApJ*, 561, 146
- Crenshaw, D. M., Kraemer, S. B., Bruhweiler, F. C., & Ruiz, J. R. 2001, *ApJ*, 555, 663
- Crenshaw, D. M., Kraemer, S. B., Turner, T. J., Collier, S., Peterson, B. M., Brandt, W. N., Clavel, J., George, I. M., Horne, K., Kriss, G. A., Mathur, S., Netzer, H., Pogge, R. W., Pounds, K. A., Romano, P., Shemmer, O., & Wamsteker, W. 2001, *ApJ*, 566, 187
- De Zotti, G., & Gaskell, C. M. 1985, *A&A*, 147, 1
- Draine, B. T. & Salpeter, E. E. 1979, *ApJ*, 231, 77
- Dultzin-Hacyan, D., and Ruano, C. 1996, *A&A*305, 719
- Fischera, Jg., Tuffs, R. J., Völk, H. J. 2002, *A&A*, 395, 189
- Fizpatrick, E. L., & Massa, D. 1988, *ApJ*, 328, 734

- Francis, P. J., Hewett, P. C., Foltz, C. B., Chaffee, F. H. 1992, *ApJ*, 398, 476
- Gaskell, C. M., Doroshenko, V. T., Klimek, E. S., Crowley, K. A., George, T. A., Grove, R., Hedrick, C. H., Hiller, M. E., Peterson, B. W., & Poulsen, M. A. et al., 2003, in preparation
- Gaskell, C. M. & Klimek, E. S. 2003, *A&ApT*, 23, 22, 661.
- Goodrich, R. W. 1989, *ApJ*, 340, 190
- Goosmann, R. W. 2002, Diplomarbeit thesis, Univ. Hamburg
- Gordon, K. D., Hanson, M. M., Clayton, G. C., Rieke, G. H., & Misselt, K. A. 1999, *ApJ*, 519, 165
- Gordon, K. D., & Clayton, G. C. 1998, *ApJ*, 500, 816
- Grandi, S. A. 1983, *ApJ*, 268, 591
- Hall, P. S. et al., 2002, *ApJS*, 141, 267
- Imanishi, M. 2001, *AJ*, 121, 1927
- Kembhavi, A. 1997, *MNRAS*, 264, 683
- Korista, K. T. & Goad, M. R. 2001, *ApJ*, 553, 695
- Kriss, G. A., Peterson, B. M., Crenshaw, D. M., Zheng, W. 2000, 535, 58
- Laor, A., Draine, B. T, 1993, *ApJ*, 402, 441
- Kriss, G. A. & Canizares, C. R. 1985, *ApJ*, 297, 177
- Krolik, J. H. & Begelman, M. C. 1988, *ApJ*, 329, 702
- Maccacaro, T., Perola, G. C., & Elvis, M. 1982, *ApJ*, 257, 47

- Maiolino, R., Marconi, A., & Oliva, E. 2001a, *A&A*, 365, 37
- Maiolino, R., Marconi, A., Salvati, M., Risaliti, G., Severgnini, P., Oliva, E., La Franca, F., & Vanzi, L. 2001b, *A&A*, 365, 28
- Malkan, M. A. 1984, in “X-Ray and UV Emission from Active Galactic Nuclei”, Max-Planck Inst. Reports, Vol. 184, p. 121-128)
- Maoz, D., Korista, K. T., Shapovalova, A. I., Shields, J. C., Smith, P. S., Thiele, U., Wagner, R. M. 1993, *ApJ*, 404, 576
- Martel, A. R. 1998, *ApJ*, 508, 657
- Mathis, J. S. 1990, *ARA&A*, 28, 37
- Mathis, J. S., Rumpl, W., & Nordsiek, K. H. 1977, *ApJ*, 217, 425 (MRN)
- McKee C. F., & Petrosian V. 1994, *ApJ*, 189, 17
- Miller, J. S., Goodrich, R., & Mathews, W. G. 1991, *ApJ*, 378, 47.
- Misselt, K. A., Clayton, G. C., & Gordon, K. D. 1999, *ApJ*, 515, 128
- Mushotzky, R. F. & Wandel, A. 1989, *ApJ*, 339, 674
- Netzer H. 1985, *ApJ*, 289, 451
- Netzer H., & Davidson K. 1979, *MNRAS*, 187, 871
- Netzer H., Brotherton M. S., Wills B. J., Han M. S., Wills D., Baldwin J. A., Ferland G. J., & Browne I. W. A. 1995, *ApJ*, 448, 27
- Ogle, P. M., Brookings, T., Canizares, C. R., Lee, J. C., & Marshall, H. L. 2003, *A&A*, 402, 849.

- Oknyanskij, V. L., Horne, K., Lyuty, V. M., Sadakane, K., Honda, S., & Tanabe, S. in *Active Galactic Nuclei, from Central Engine to Host Galaxy*, eds. S. Collin, F. Combes and I. Shlosman. ASP Conf. Ser, Vol. 290, p. 119
- Perola, C. et al. 1982, MNRAS, 200, 293
- Pitman K. M., Clayton G. C., & Gordon K. D. 2000, PASP, 112, 537
- Reichert, G. A., Mason, K. O., & Bowyer, S. 1981, BAAS, 12, 849.
- Reichert, G. A., Mushotzky, R. F., Holt, S. S., & Petre, R. 1985, ApJ, 296, 69
- Rieke G. H., & Lebofsky M. J. 1985, ApJ, 288, 618
- Risaliti, G., Elvis, M., & Nicastro, F. 2002, ApJ, 571, 234
- Sambruna, R. M., Eracleous, M., & Mushotzkym, R. F. 1999, ApJ, 526, 60
- Shastri, P. 1991, MNRAS, 249, 640
- Wandel, A. & Petrosian, V. 1988, ApJ, 329, L11
- Ward M. J., Elvis M., Fabbiano G., Carleton N. P., Willner S. P., & Lawrence A. 1987, ApJ, 315, 74
- Ward, M. J. & Morris, S. L. 1984, MNRAS, 207, 867
- Weingartner J. C., & Draine B. T. 2001, ApJ, 548, 296
- Wills, B. J. 1999, in *Introduction to Unified Schemes Quasars and Cosmology*, ASP Conference Series 162, ed. G. J. Ferland & J. A. Baldwin. Astronomical Society of the Pacific (San Francisco), p.101

Zamorani, G., Henry, J. P., Maccacaro, T., Tananbaum, H., Soltan, A., Avni, Y., Liebert, J., Stocke, J., Strittmatter, P. A., Weymann, R. J., Smith, M. G., & Condon, J. J. 1981, ApJ, 245, 357

Table 1. AGN Extinction at Major Emission Lines and Wavebands

Line	λ [\AA]	A_λ/A_V
O I	8446	0.548
H α	6563	0.813
He I	5876	0.927
V band	5500	0.994
H β	4861	1.111
He II	4686	1.143
B band	4400	1.196
He I	4471	1.183
H γ	4340	1.207
Mg II	2798	1.405
C II]	2326	1.414
C III]	1909	1.422
He II	1640	1.430
C IV	1549	1.433
O IV/Si IV	1400	1.439
O I	1304	1.444
N V	1240	1.447
Ly α	1216	1.449
O IV	1034	1.462

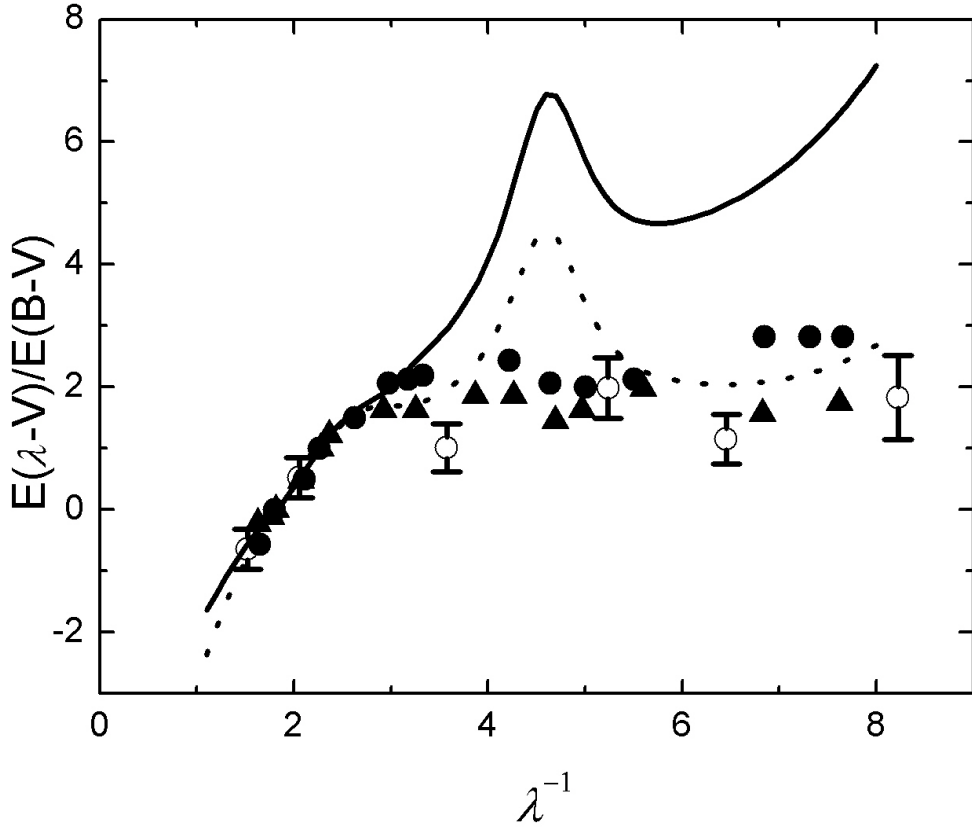


Fig. 1.— Reddening curves based on the Baker & Hunstead (1995, 1996) data subsets for composite spectra. Filled triangles are from comparing $\mathfrak{R} \geq 1$ with $\mathfrak{R} \leq 0.1$ and filled circles are from comparing $0.1 \leq \mathfrak{R} < 1$ with CSS. The open circles represent average BLR extinction values between face-on ($\mathfrak{R} \geq 1$) and edge-on ($\mathfrak{R} < 0.1$, CSS) objects. Theoretical reddening curves derived from CCM89 for $R_V = 5.3$ and $R_V = 3.1$ are shown as dashed and solid curves respectively.

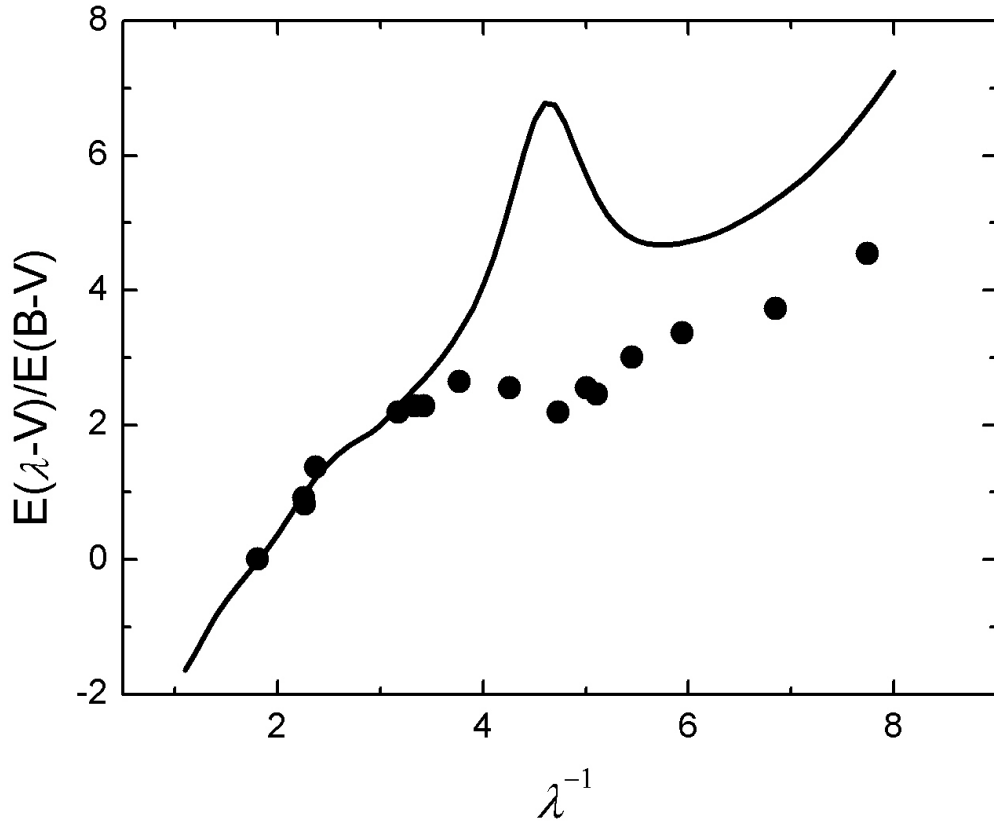


Fig. 2.— Observational Reddening curve based on the Baker & Hunstead data for the composite spectrum $\mathfrak{R} \geq 1$ to LBQS (circles). Computed reddening curve derived from CCM89 for $R_V = 3.1$ (solid curve).

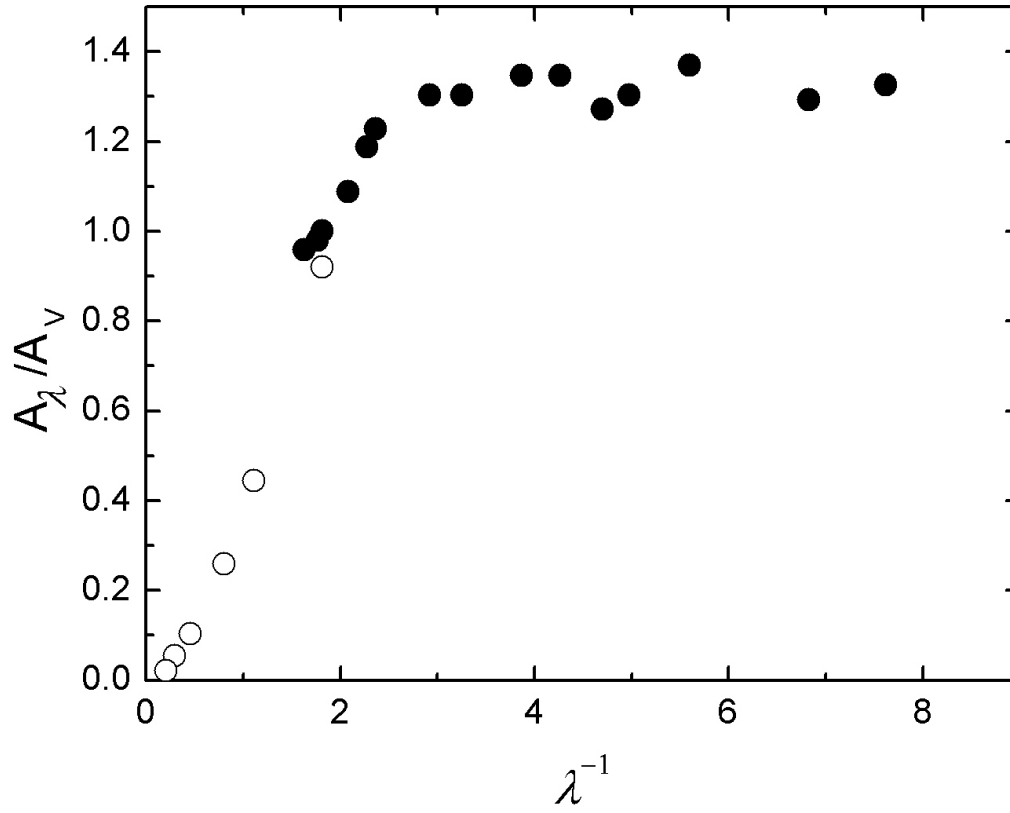


Fig. 3.— Optical and UV reddening curve between the composite spectra $0.1 \leq \mathfrak{R} < 1$ and CSS (filled circles) with an extrapolation into the IR based on Rieke & Lebofsky (open circles).

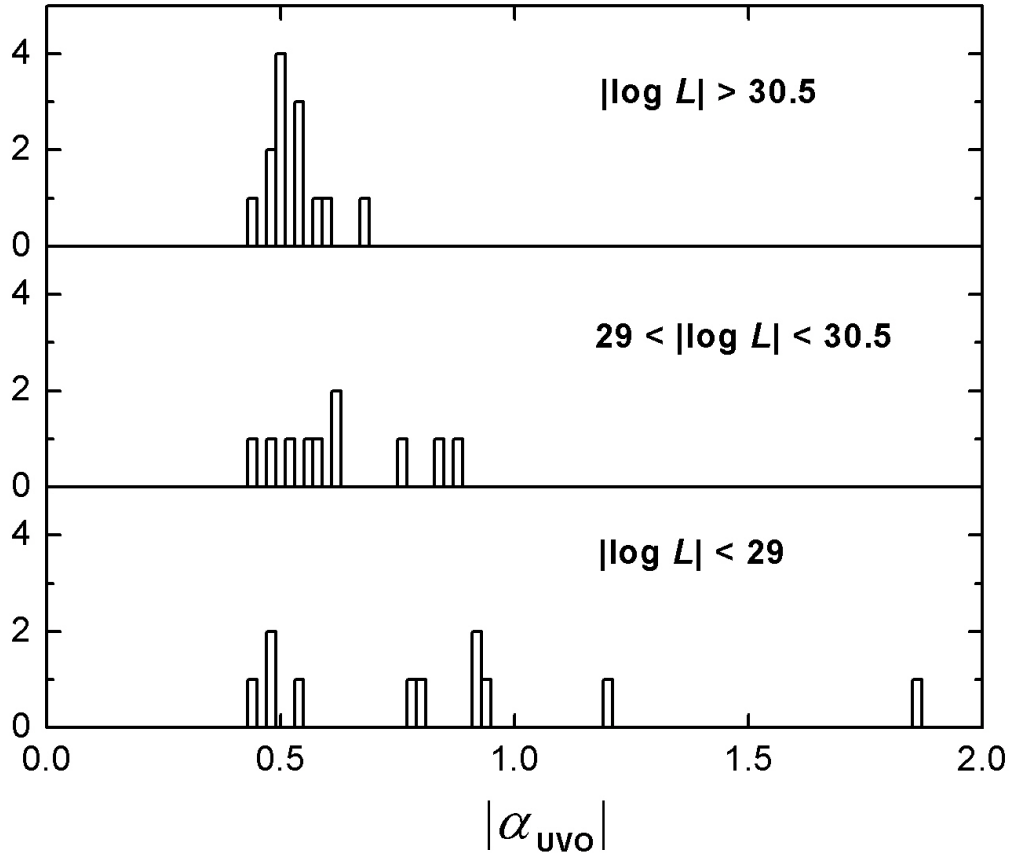


Fig. 4.— Number distribution of α_{UVO} for AGNs in three different luminosity ranges, $|\log L| > 30.5$ (a), $29 < |\log L| < 30.5$ (b) and $|\log L| < 29$ (c)

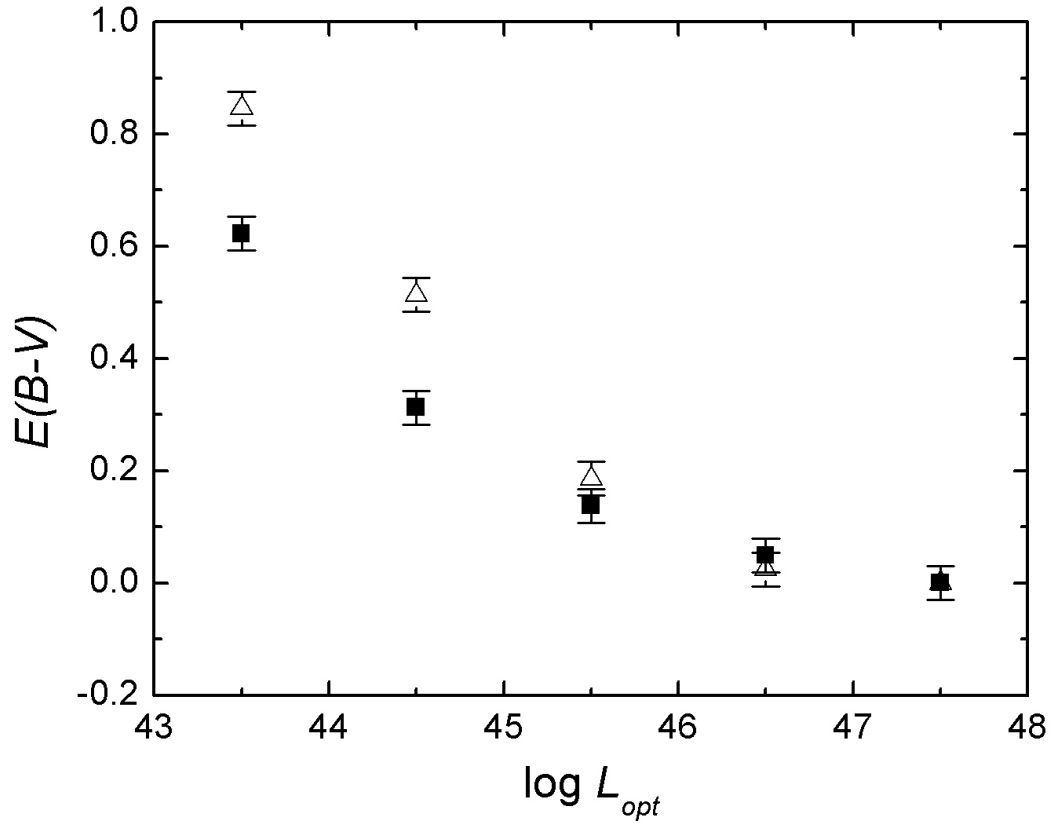


Fig. 5.— The reddening, ($E(B-V)$), of AGNs as a function of observed optical luminosity (ergs s^{-1}). The solid squares are reddenings derived from the $\lambda 1600$ to $\lambda 4200$ spectral index, the open triangles are the reddenings derived from the $\lambda 4200$ to $\lambda 7000$ spectral index.

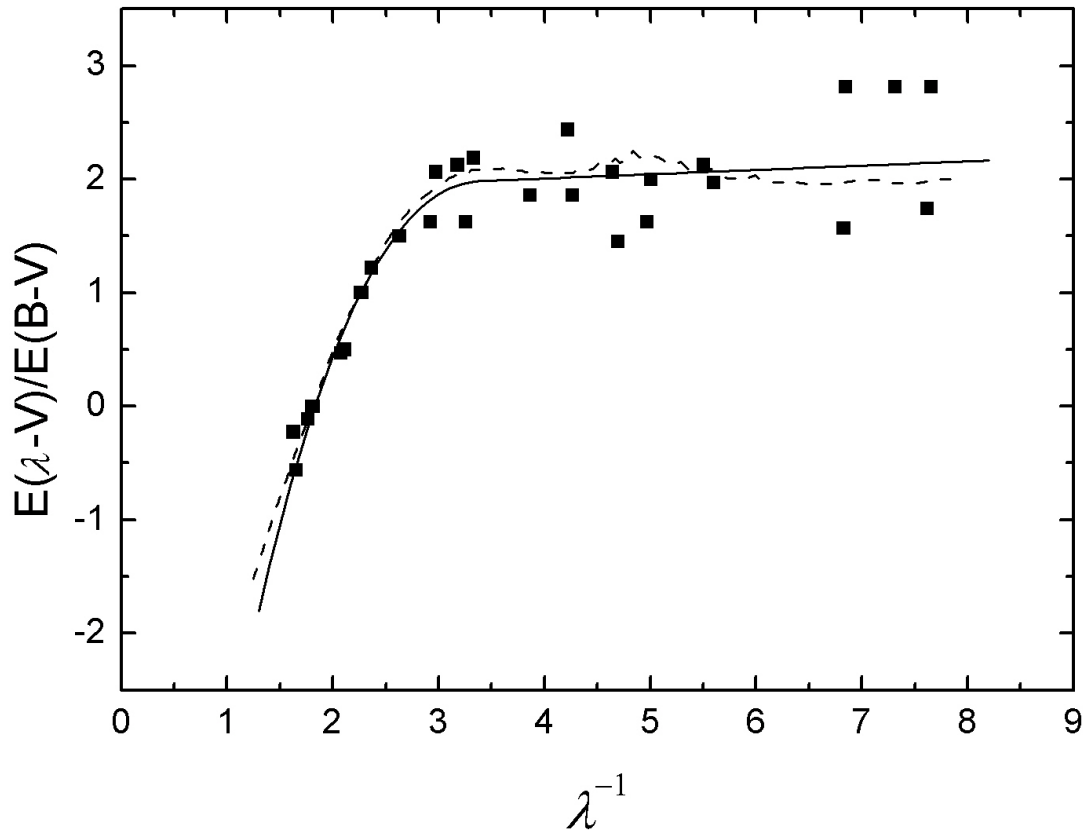


Fig. 6.— AGN extinction curves (squares) plotted together with a model curve derived from Mie theory computations (dotted line, see section 4.2) and the analytical fit given in the Appendix (solid line)